Supporting Information

**An Interesting Possibility of Forming Special Hole Stepping Stones by High-Stacking Aromatic Rings in Proteins: Three-π Five-Electron and Four-π Seven-Electron Resonance Bindings**

Xin Li[#], Weichao Sun[#], Xin Qin, Yuxin Xie, Nian Liu, Xin Luo, Yuanying Wang, Xiaohua Chen*

Chongqing Key Laboratory of Theoretical and Computational Chemistry, School of Chemistry and Chemical Engineering,

Chongqing University, Chongqing, 401331, P.R. China

National-Municipal Joint Engineering Laboratory for Chemical Process Intensification and Reaction, Chongqing University,
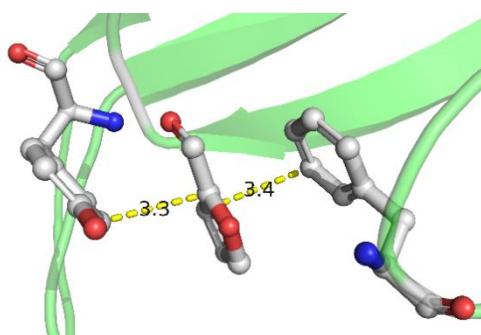
Chongqing, 401331, P.R. China

1. Three-π and four-π structures in protein crystal structures
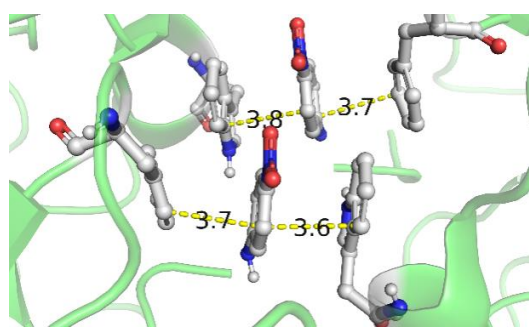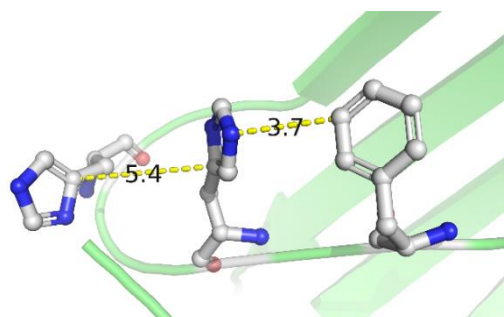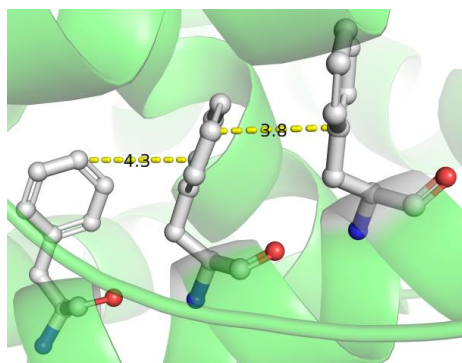

1RMH: F60–NIT6–W121
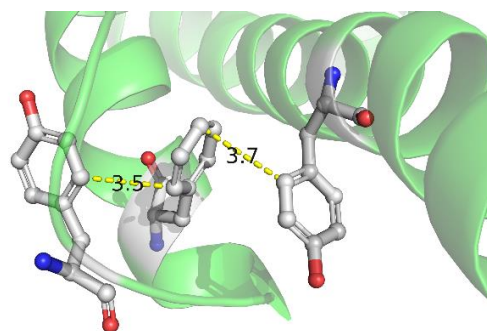
1HJN: Y169–F175–Y218

5HJB: Y78-FOA101-F59

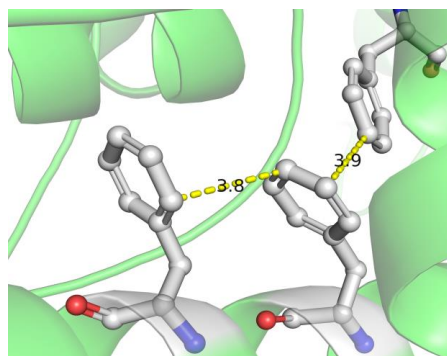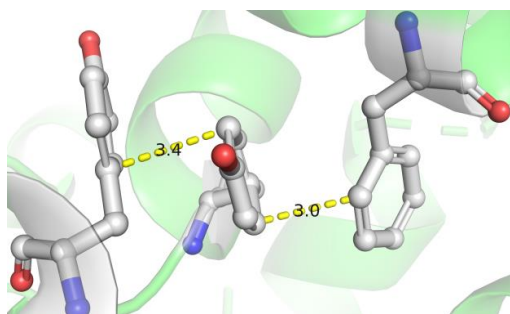6MIL:H116-F105-H107

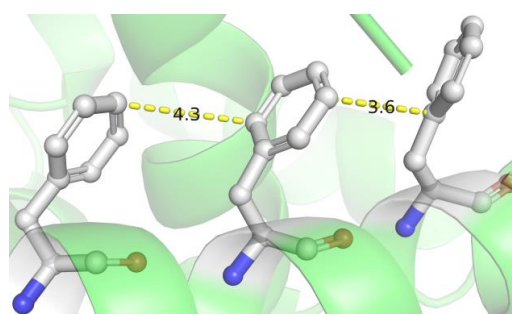[#]Li and Sun contributes equally to this work. *The corresponding authors: Xiaohua Chen, chxh7@cqu.edu.cn
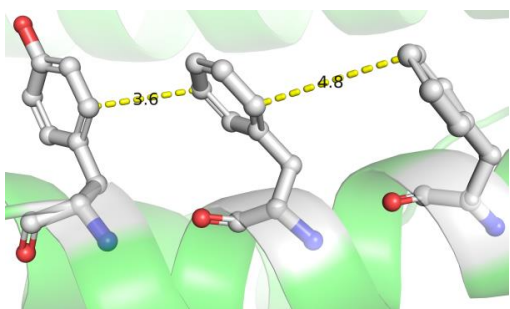
2B11:F266-F262-F198

2B11:F758-F762-F766

2PCB:F258-F262-F266

2PCB:Y36-Y42-F91

2PCB:F23-F286-Y284
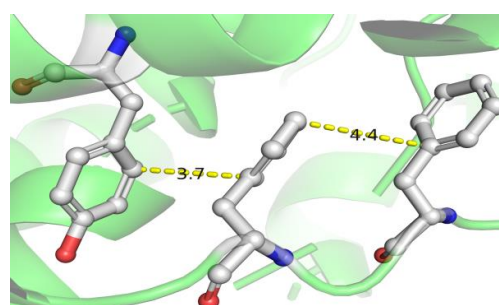
3U2M:Y140-F132-F136
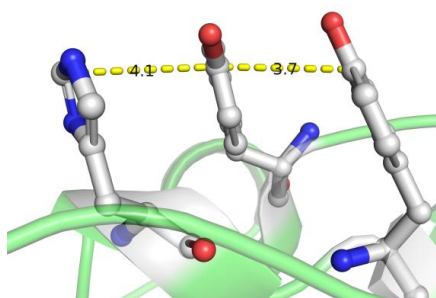
3W5V:H78-Y23-Y80
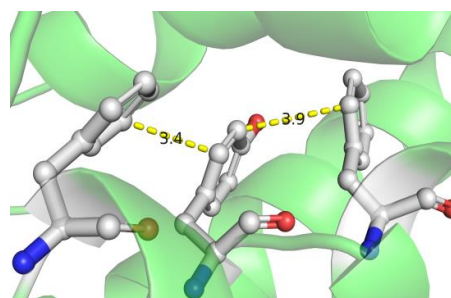
3W9C:F150-Y154-F158

Figure S1. The three-π stacking structures in the crystal structures of proteins by surveying the protein data bank (PDB). The markings under the picture include the code of PDB and three aromatic amino acids taking part in forming three-π cluster. Notwithstanding the aromatic rings are not always parallelly aligned well, the movement of proteins may promote the transient formation of the three-π stacking structures to accept a hole.

5HJB:H15-F105-H107-Y102

5HJC:F334-F384-F408-F412

2BNP:F266-W127-W130-F123

1XZW:F255-F306-F265-F755
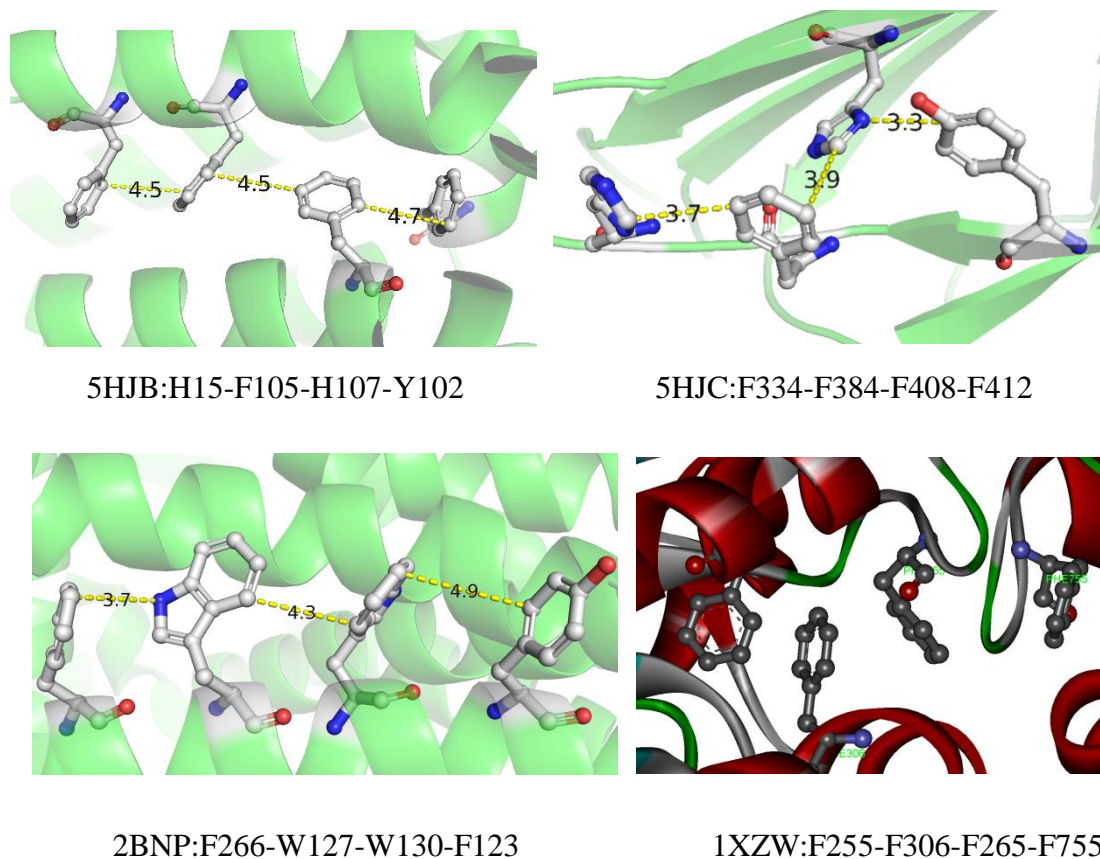
Figure S2. Four examples of four-π stacking structures in the crystal structures of proteins by surveying the protein data bank (PDB).

2. Comparison of different DFT functionals

FFF   SOMO   HDMO   HDMO-3

YYY   SOMO   HDMO   HDMO-1

FFFF   SOMO   HDMO

HDMO-1   HDMO-4

YYYY   SOMO   HDMO

HDMO-1   HDMO-2
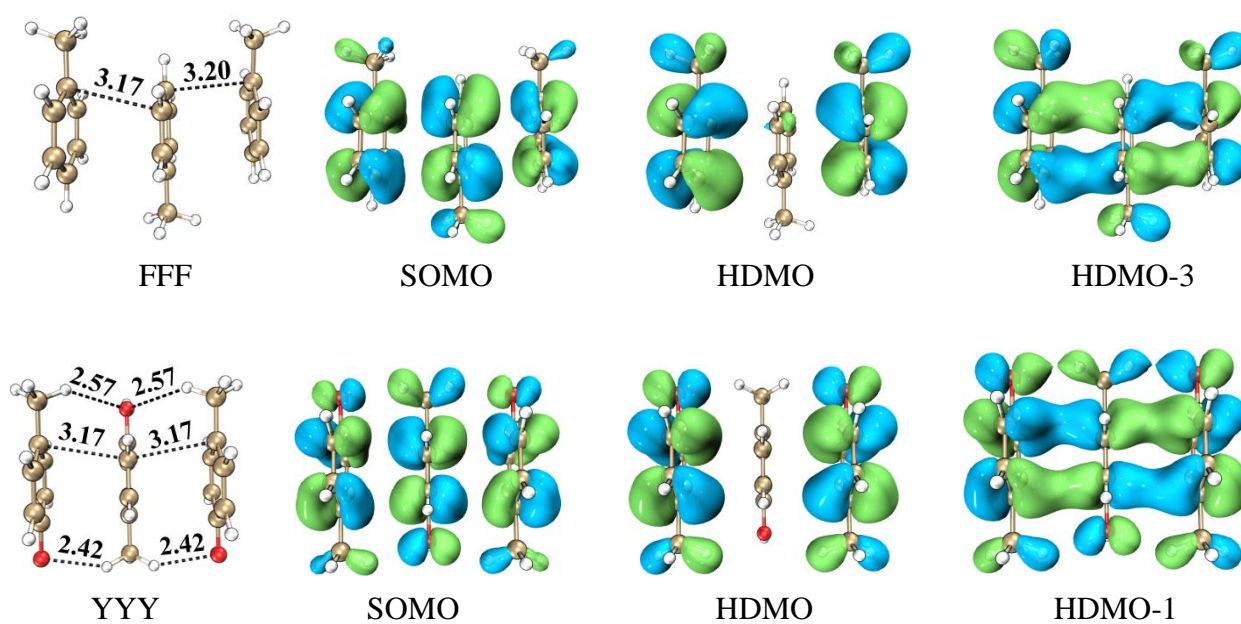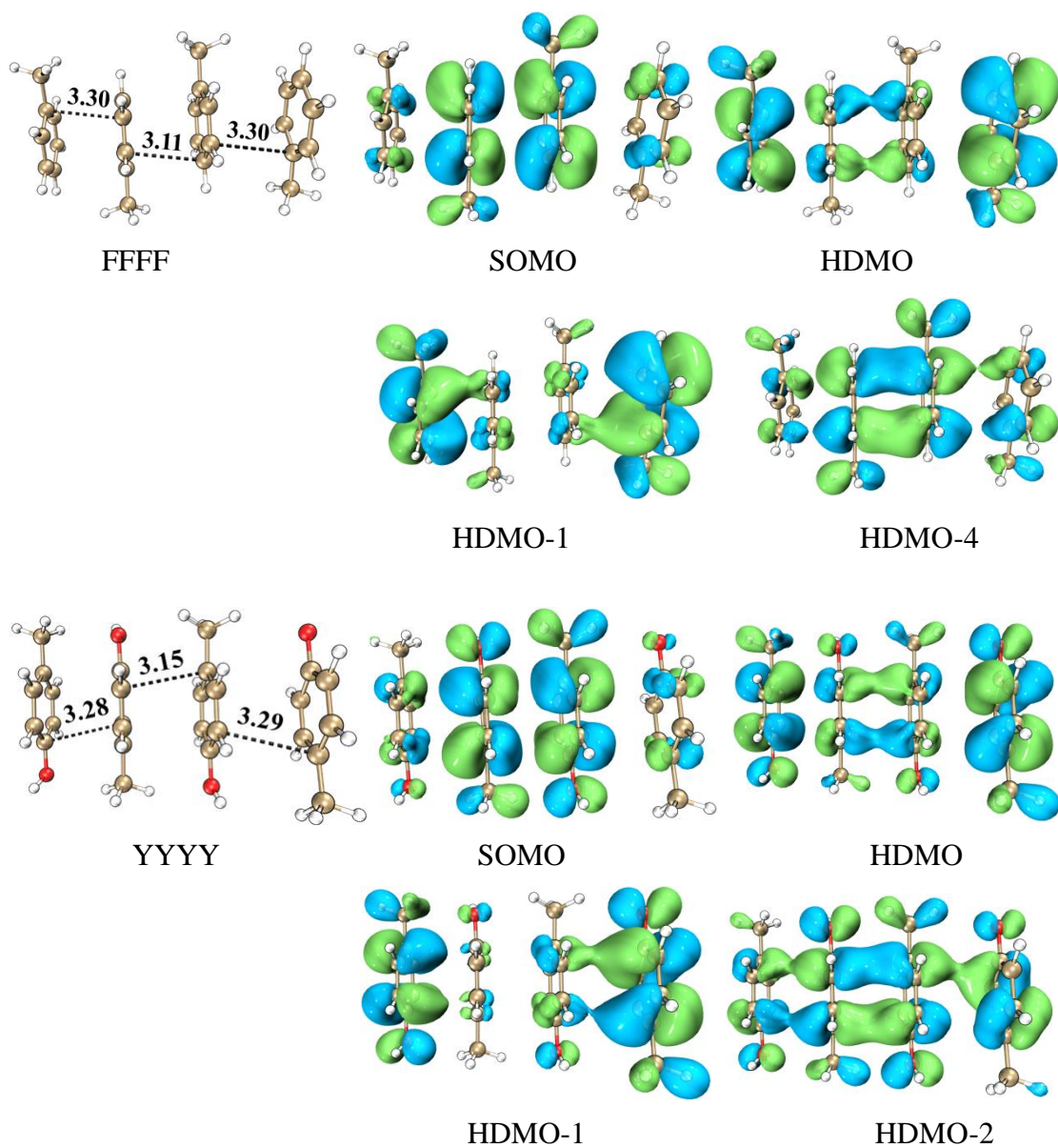
Figure S3. The formations of three-π five-electron bindings in YYY and FFF and four-π seven-electron bindings in YYYY and FFFF confirmed by the ωB97XD/6-31+g(d,p) optimization.

Figure S4. The YYY and FFF three-π and YYYY four-π systems are optimized by the CAM-B3LYP/6-31+g(d,p) method. It should be noted that the distances between the neighboring aromatic rings in YYY, FFF and YYYY obtained from the long-range corrected CAM-B3LYP functional are larger than the corresponding distances obtained from the M06-2X functional.

3. Tables

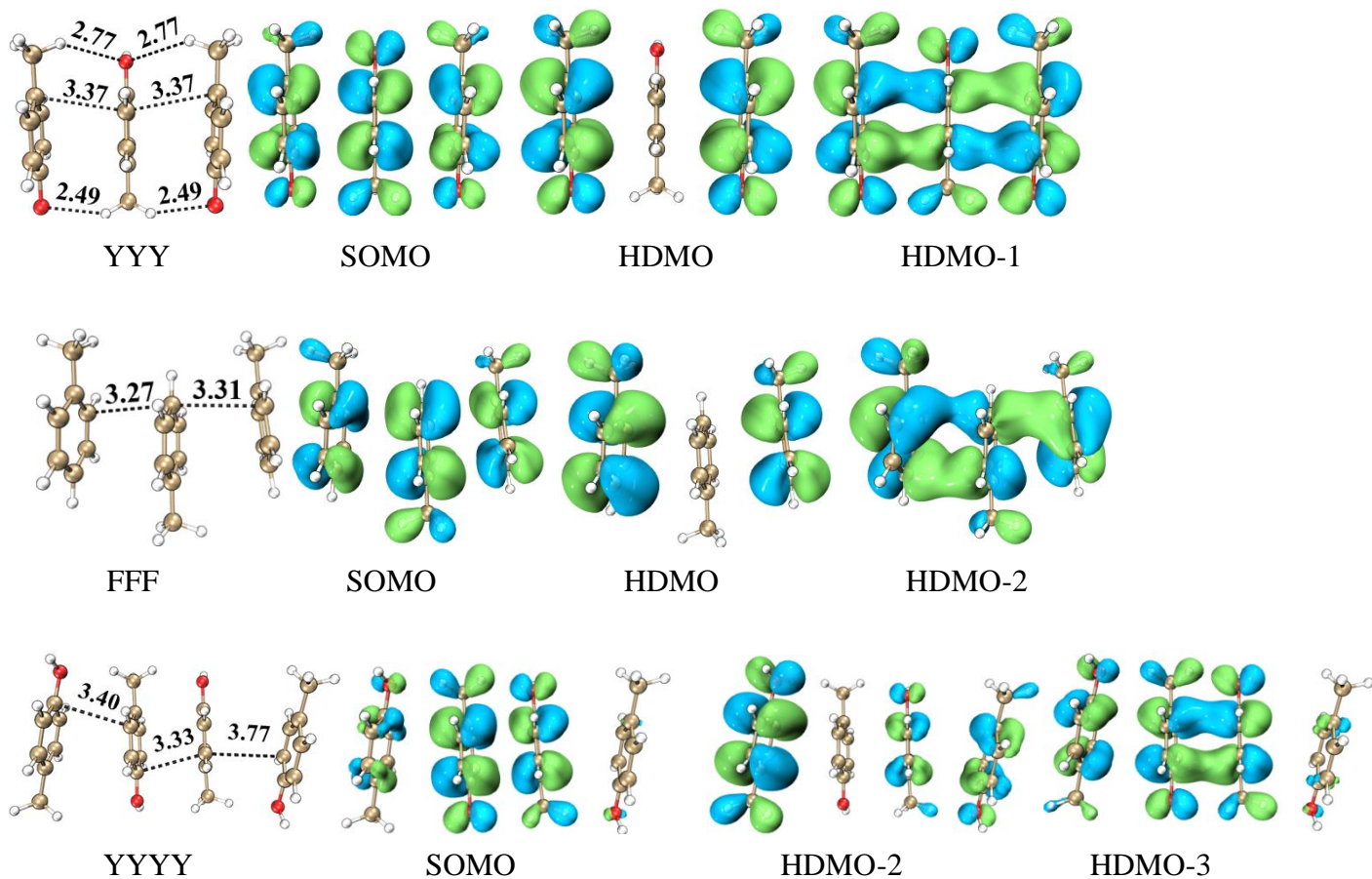**Table S1.** Shortest Distance between the Neighboring Aromatic Rings (d_{min}, in Å), Binding Energy (BE, in kcal/mol), Vertical Ionization Potential (IP_v, in eV) and Decreasing Value of IP (ΔIP, in eV) compared to the corresponding monomer for all the YYY, FFF, YYYY stacking systems obtained by three functionals, M06-2X, ωB97XD and CAM-B3LYP.

Species		FFF	YYY	FFFF	YYYY
M06-2X	d_{min}(Å)	3.18/3.19	3.11/3.12	3.31/3.13/3.23	3.16/3.29/3.77
	BE(kcal/mol)	11.57	12.23	8.03	10.42
	IP(eV)	7.57	7.02	7.42	6.74
	ΔIP(eV)	1.07	0.88	1.22	1.16
ωB97XD	d_{min}(Å)	3.17/3.20	3.17/3.17	3.30/3.11/3.30	3.28/3.15/3.29
	BE(kcal/mol)	11.53	12.64	8.78	10.01
	IP(eV)	7.42	6.87	7.26	6.62
	ΔIP(eV)	1.42	1.33	1.58	1.58
CAM-B3LYP	d_{min}(Å)	3.27/3.31	3.37/3.37	/	3.40/3.33/3.77
	BE(kcal/mol)	4.25	5.16	/	3.31
	IP(eV)	7.58	7.03	/	6.79
	ΔIP(eV)	1.29	1.22	/	1.46

Note: As shown in Figure S3 and S4, the single occupied molecular orbitals (SOMO) delocalize over the three parallel aromatic rings for the YYY and FFF three-π stacking systems, which indicates that the three-π, five-electron bindings can form in the three close aromatic rings according to the calculations of the three functionals, M06-2X, ωB97XD and CAM-B3LYP. One trend that has been observed is that CAM-B3LYP gives the close distances between the neighboring rings that are typically longer than those of M06-2X, while wB97XD gives the close distances that are shorter than those of M06-2X. This may be attributed to that the CAM-B3LYP functional only contains the long-range correction and the ωB97XD functional includes both the long-range and dispersion corrections. Then, the former underestimates the binding strengthen between two neighbor aromatic rings. The corresponding binding energies, as shown in Table s1, also confirms this conjecture. More importantly, the trend in the vertical ionization potential (IP_v) of YYY and FFF are well consistent for the three functionals, as shown in Table S1. These consistences confirms that it is suitable to use M06-2X to examine the relay function of the high π-stacking structures in proteins.

Table S2. Vertical Ionization Potential (IPv, in eV) and Decreasing Value of IPv ($_\triangle$IP, in eV) compared to the corresponding monomer in the three continuum solvents, including diethyl ether (ε= 4.335), dichloroethane (DCE）(ε= 10.36) and water (ε= 78.36) obtained at the B3LYP/6-311+G(d,p) for all the structures.

Species	F	Y	H	W	YYY	FFF	HHH	YFY	YHY
IPv-ether	7.40	7.00	6.62	6.32	5.83	6.37	5.37	6.11	5.68
△IP-ether	\	\	\	\	1.17	1.03	1.26	0.89	0.94
IPv-DCE	7.12	6.73	6.32	6.07	5.61	6.15	5.16	5.91	5.48
△IP-DCE	\	\	\	\	1.12	0.97	1.16	0.82	0.84
IPv-water	6.94	6.56	6.14	5.91	5.48	6.01	5.03	5.79	5.36
△IP-water	\	\	\	\	1.08	0.93	1.10	0.78	0.78

Species	YWY	FYY	WYY	HYY	FYF	FHF	FFY	HFH	HYH
IPv-ether	5.28	5.84	5.77	5.63	5.86	5.72	6.05	6.07	5.81
△IP-ether	1.04	1.16	0.55	0.99	1.14	0.90	0.95	0.56	0.81
IPv-DCE	5.07	5.62	5.58	5.43	5.64	5.49	5.82	5.85	5.58
△IP-DCE	1.00	1.11	0.50	0.89	1.09	0.84	0.91	0.48	0.74
IPv-water	4.93	5.49	5.46	5.31	5.49	5.34	5.68	5.71	5.44
△IP-water	0.98	1.08	0.46	0.83	1.07	0.79	0.89	0.43	0.70

Species	FHY	FYH	FWY	YFH	WHW	FFFF	YYYY	HHHH	YFHY
IPv-ether	5.76	5.89	5.31	6.05	5.09	6.30	5.67	5.30	5.74
△IP-ether	0.86	0.73	1.01	0.57	1.23	1.10	1.34	1.33	0.88
IPv-DCE	5.54	5.66	5.09	5.86	5.34	6.09	5.47	5.11	5.54
△IP-DCE	0.78	0.66	0.98	0.47	0.73	1.03	1.26	1.22	0.78
IPv-water	5.40	5.52	4.95	5.74	5.22	5.96	5.35	4.99	5.42
△IP-water	0.73	0.61	0.96	0.40	0.70	0.98	1.22	1.15	0.72

Species	FYYY	FYFY	YFFY	FFFFF	YYYYY	HHHHH	FFFFFF	YYYYYY

IPᵥ-ether	5.73	5.82	6.26	6.28	5.67	5.36	6.27	5.63
$\triangle$IP-ether	1.27	1.18	0.74	1.12	1.33	1.26	1.13	1.37
IPᵥ-DCE	5.53	5.61	6.08	6.07	5.48	5.18	5.92	5.46
$\triangle$IP-DCE	1.20	1.12	0.64	1.04	1.25	1.15	0.81	1.27
IPᵥ-water	5.40	5.48	5.98	5.94	5.36	5.06	5.94	5.34
$\triangle$IP-water	1.16	1.09	0.59	1.00	1.21	1.07	1.00	1.22

Species	YYY-p	FYY-p	HYY-p	YHY-p	FHF-p	FHY-p	YYYY-p	FFFF-p	YFYY-p
IPᵥ-ether	5.81	5.93	5.75	5.89	5.93	5.91	5.90	5.90	5.88
$\triangle$IP-ether	1.19	1.07	0.87	0.73	0.69	0.71		1.1	1.12
IPᵥ-DCE	5.62	5.74	5.58	5.72	5.74	5.73	5.74	5.74	5.69
$\triangle$IP-DCE	1.10	0.99	0.75	0.60	0.59	0.59		-0.99	1.04
IPᵥ-water	5.50	5.61	5.47	5.61	5.62	5.61	5.65	5.65	5.56
$\triangle$IP-water	1.06	0.95	0.67	0.52	0.52	0.52		0.92	1.00
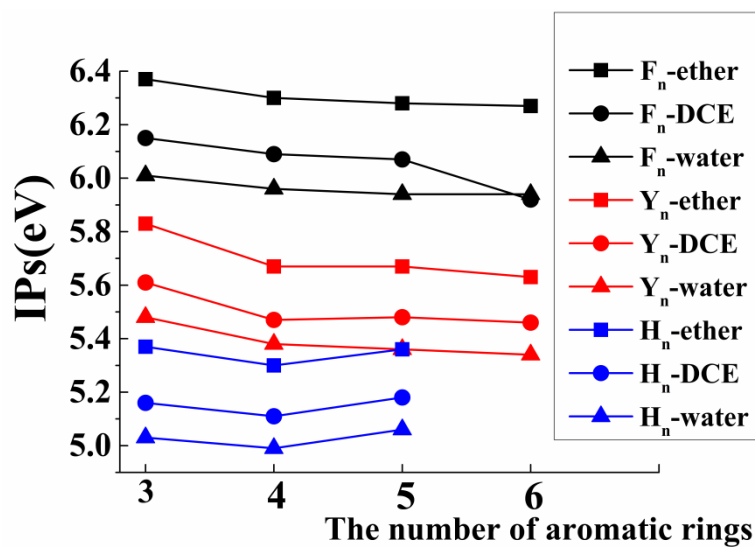
Figure S5. The changing trend of the vertical ionization energies (IP) with the increasing number of the same aromatic rings in the high π-π packing systems in different continuum solvents. Square, circular and triangle emblematize the IPs calculated in diethyl ether, dichloroethane and water, respectively.

Table S3. Shortest Distances between Each Aromatic Ring(d_{min}), Binding Energy Values(BEs), Vertical Ionization Potential (IP$_V$, in eV) and Decreasing Value of IP ($_\Delta$IP, in eV) Compared to the Corresponding Monomer.

Species	FPheF	PheFPhe	PheHPhe	FHisH	FTyrH	FHisY	FTyrY
d_{min}(Å)	3.16/3.23	3.11/3.07	2.99/2.99	3.15/2.89	3.15/2.99	3.12/2.94	3.23/2.96
BE(kcal/mol)	15.96	11.74	13.33	15.68	16.53	17.26	15.35
IP$_v$(eV)	7.42	7.61	7.05	6.70	6.80	7.04	6.86
$_\Delta$IP(eV)	0.63	0.44	1.00	1.36	1.02	1.02	0.96

Species	HPheH	HTyrH	WTyrW	TyrHTyr	TyrYTyr	YTyrY	
d_{min}(Å)	3.09/3.00	3.06/2.98	3.10/3.16	3.06/3.09	3.16/3.01	3.11/3.16	
BE(kcal/mol)	23.64	21.57	19.70	24.26	18.31	19.32	
IP$_v$(eV)	7.24	6.94	6.67	6.49	6.61	6.99	
$_\Delta$IP(eV)	0.58	0.88	0.68	1.33	1.21	0.83	

Denote: Xxx (Phe, His, Tyr and Trp) represent the structure of the amino acid has the main peptide chain.

4. Electron Transition Spectra
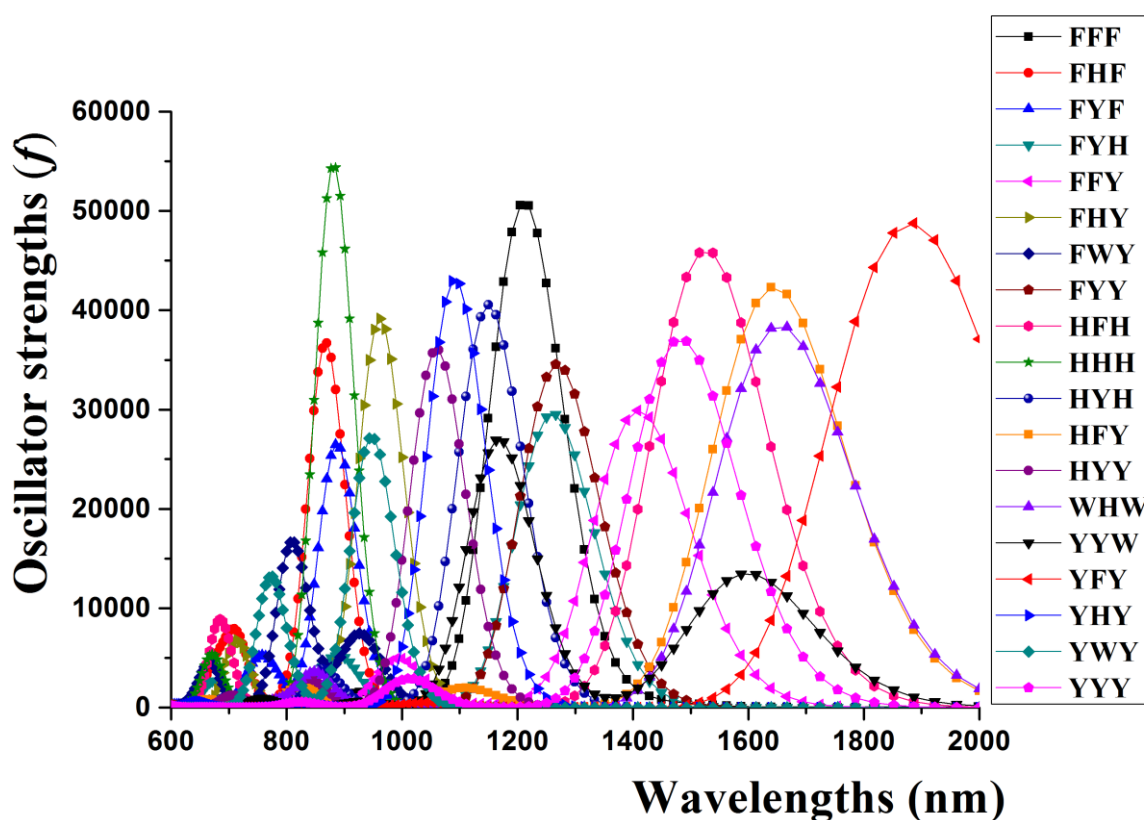
Figure S6. Electron transition spectra of 19 simple three-π structures obtained at M06-2X/6-311++G(d,p) //M06-2X/6-31+G(d,p) level of theory. The widths at half-height ($\Delta_{1/2}$) are assumed to be equal 1500 cm^{-1}. Assignments of each electron transition spectra for these models are given below the spectrum.

FXF

HXH

XYY
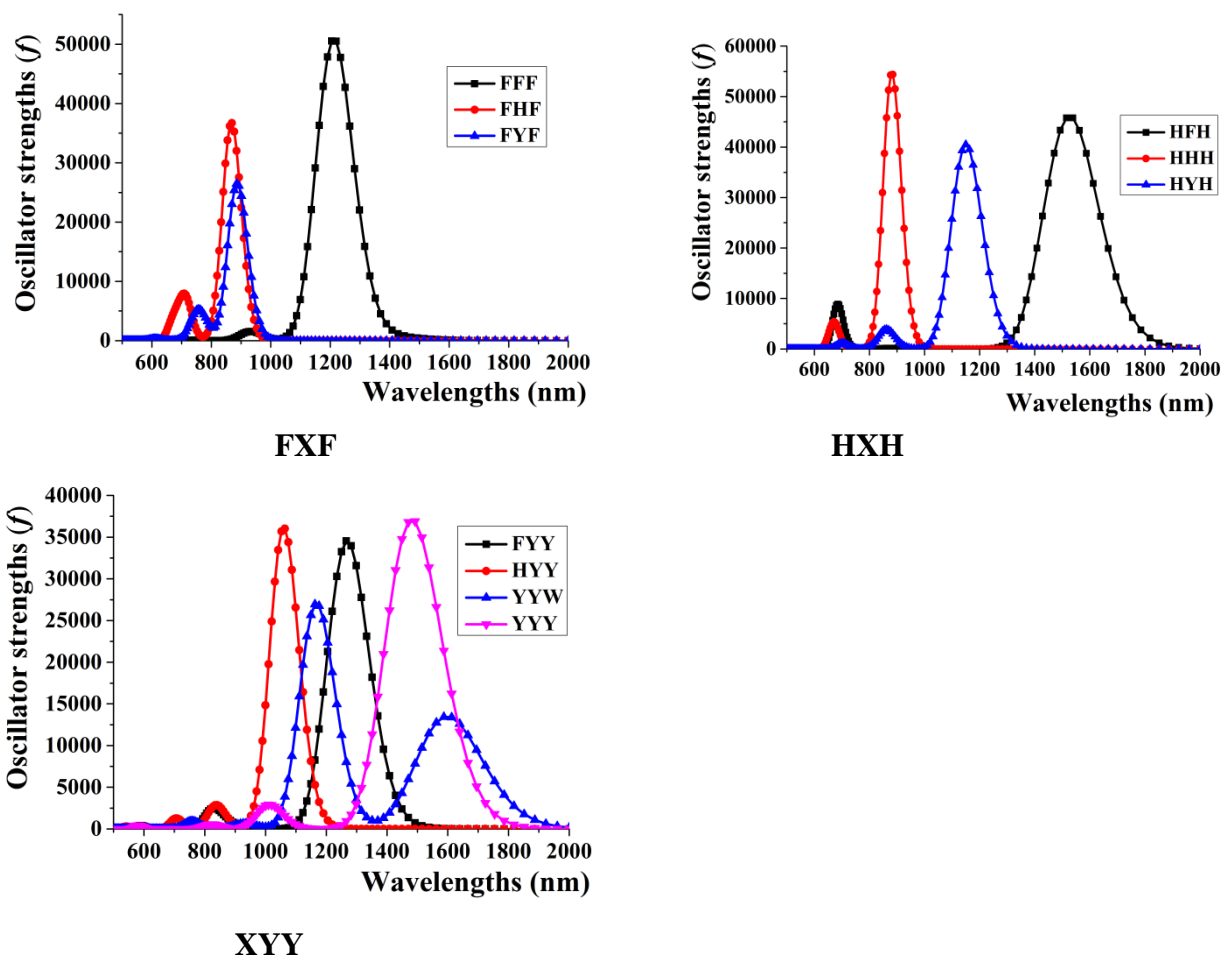
Figure S7. Two characteristic peaks $[(1\sigma)^2 \rightarrow (1\sigma^*)^1$ and $(2\sigma)^2 \rightarrow (1\sigma^*)^1]$ of the $\pi \therefore \pi : \pi \leftrightarrow \pi : \pi \therefore \pi$ resonance binding for FXF, HXH and XYY. It is shown that the maximal absorbing spectrum (λ_{max}) exhibits an obvious red shift with the increasing the size of the aromatic ring of X.
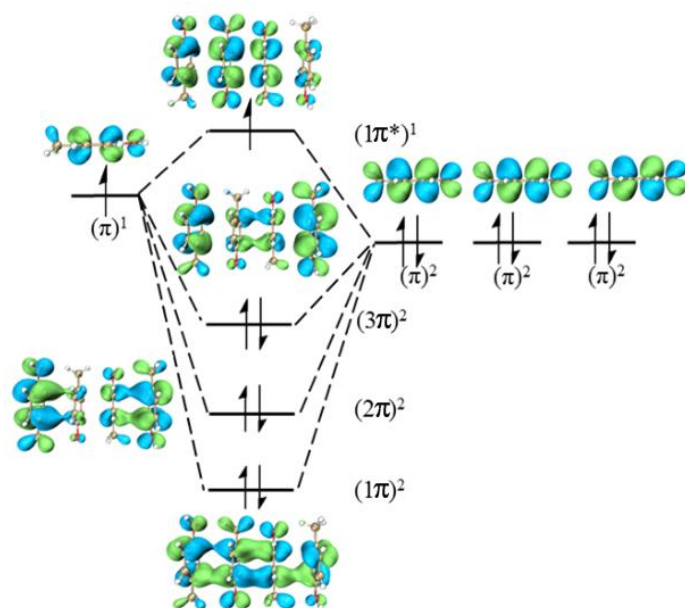
Figure S8. Exhibition of forming seven-electron binding via each highest occupied molecular orbital of the side chains of four Tyrs

5. Structures and MOs

FFF   SOMO   HDMO   HDMO-1

HHH   SOMO   HDMO   HDMO-1

YFY   SOMO   HDMO   HDMO-1

YHY   SOMO   HDMO   HDMO-1

YWY   SOMO   HDMO   HDMO-1

FYY   SOMO   HDMO   HDMO-2

| WYY | SOMO | HDMO-1 | HDMO-2 |

| HYY | SOMO | HDMO | HDMO-1 |

| FYF | SOMO | HDMO | HDMO-2 |

| FYF | SOMO | HDMO | HDMO-3 |

| FFY | SOMO | HDMO | HDMO-2 |

| HFH | SOMO | HDMO | HDMO-1 |
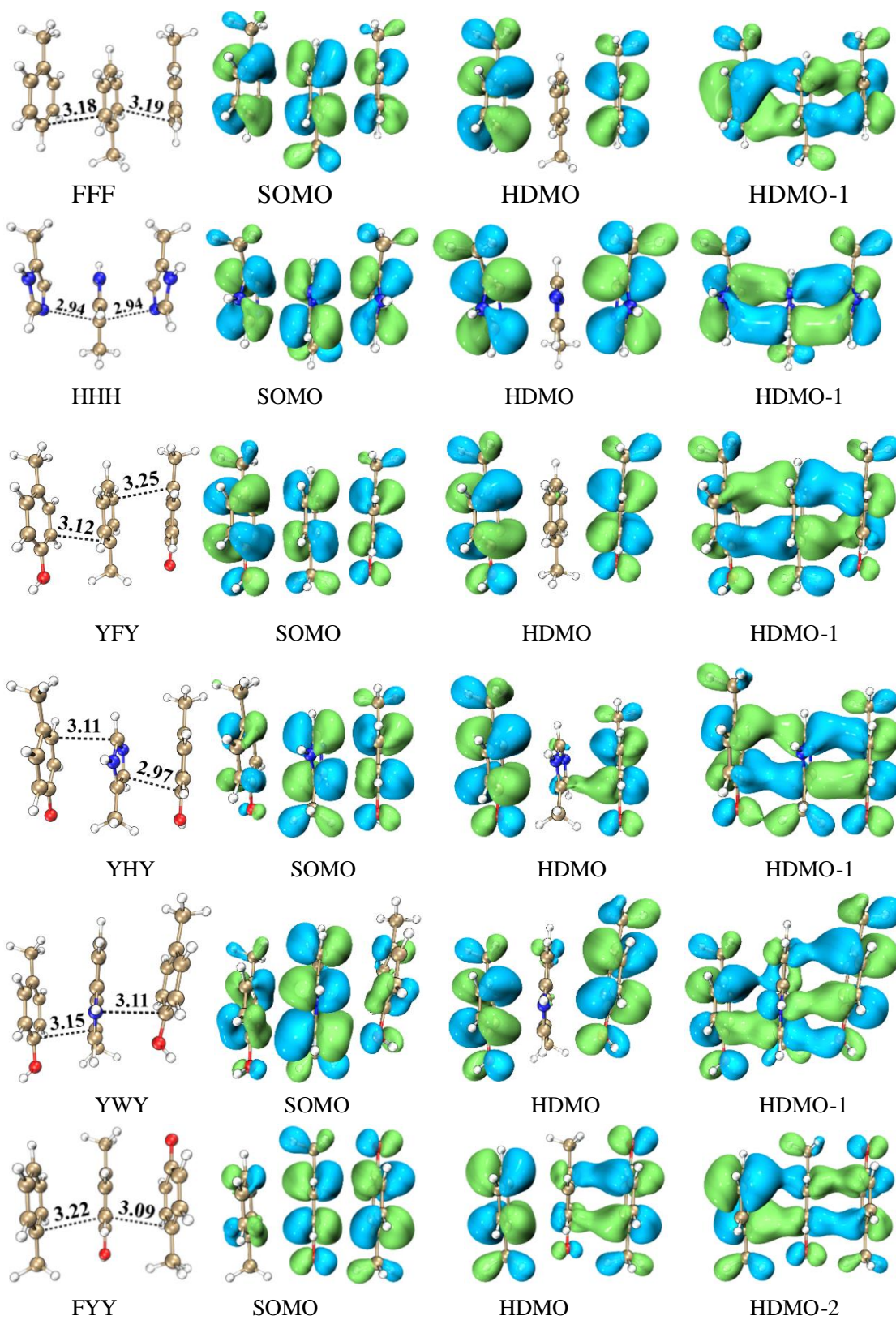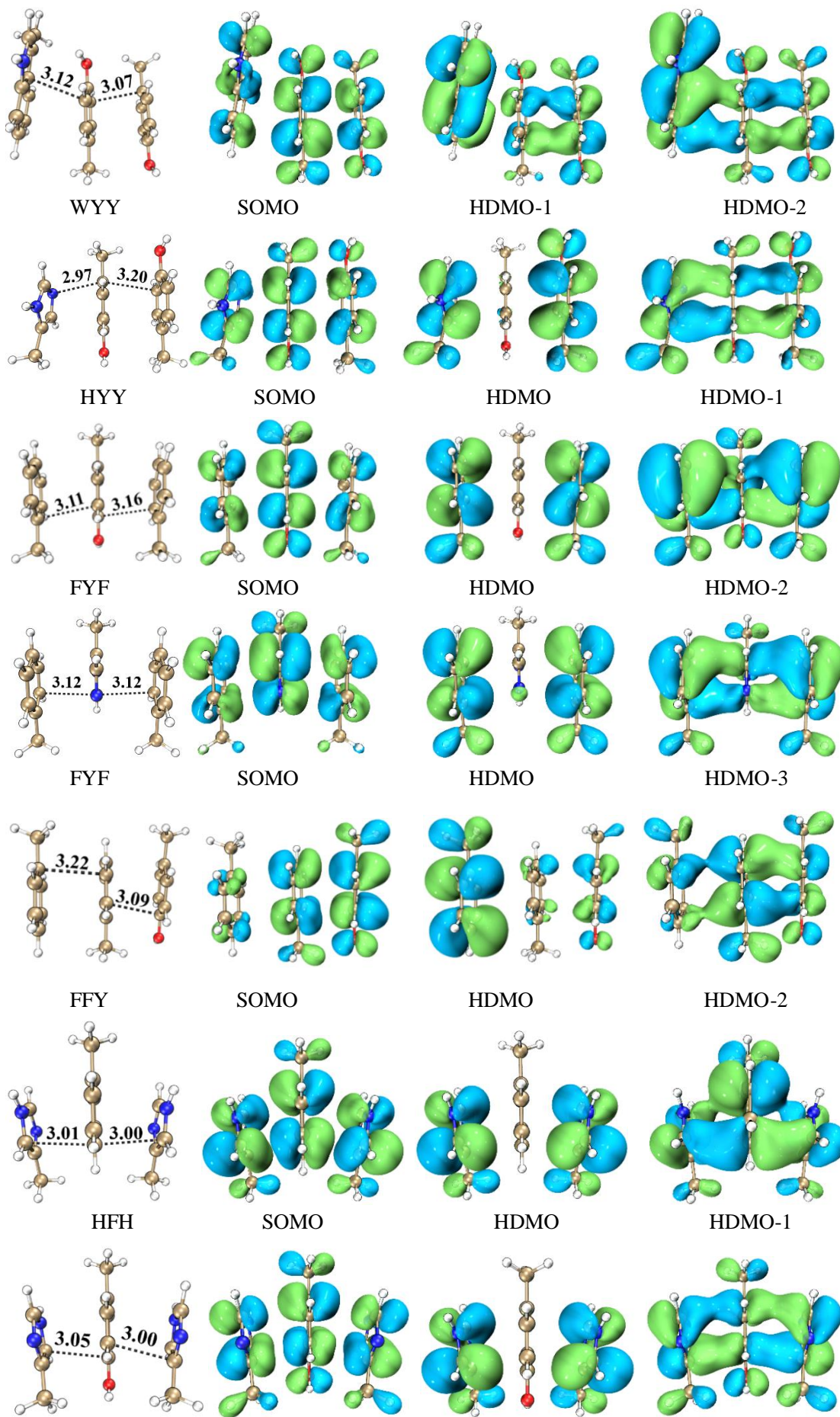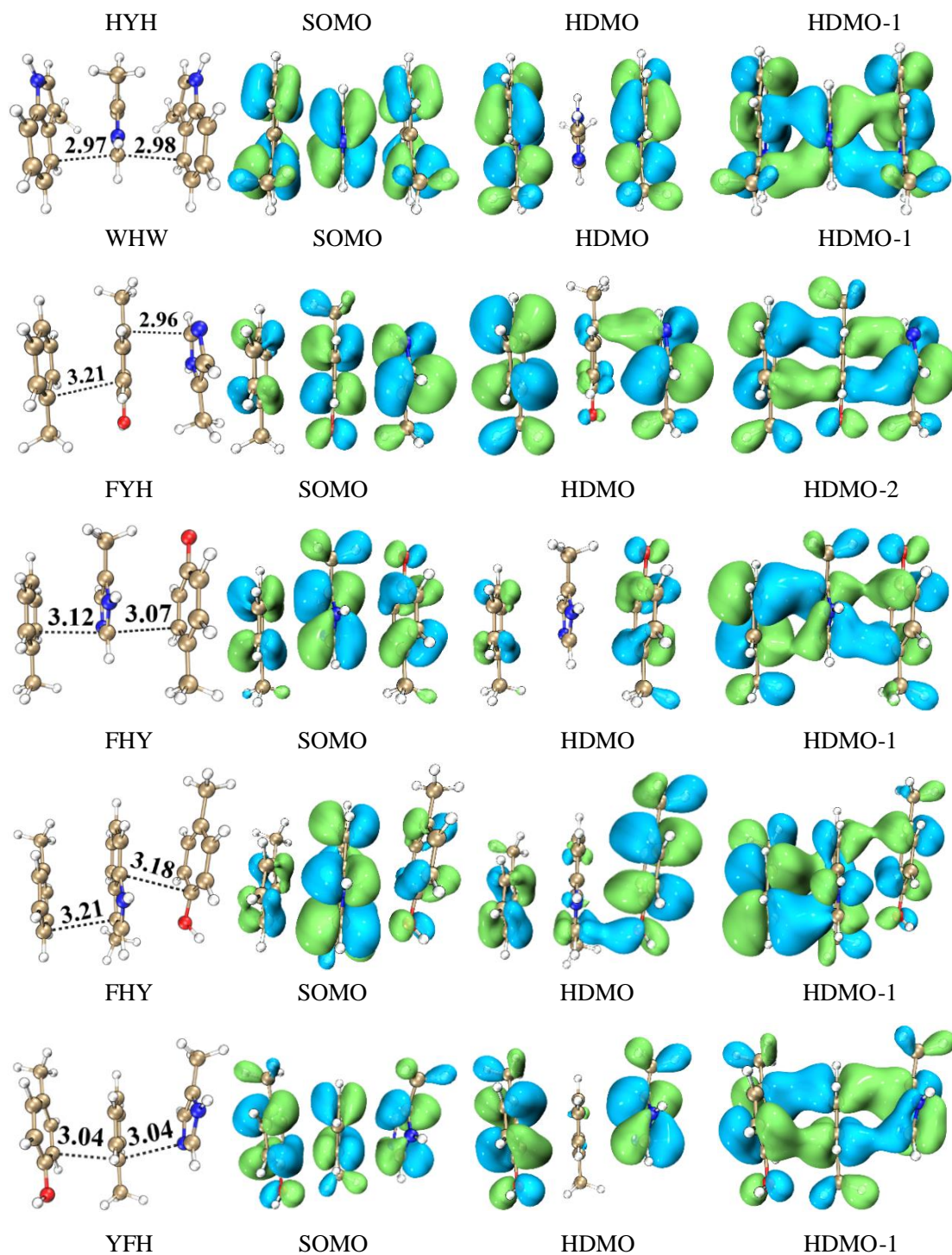
Figure S9. The structures of the three-π five-electron bindings for simple models with the corresponding SOMO, HDMO and HDMO-X.
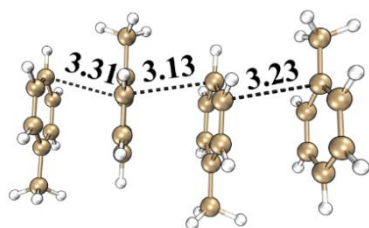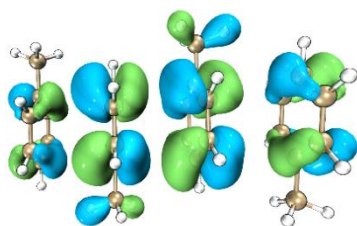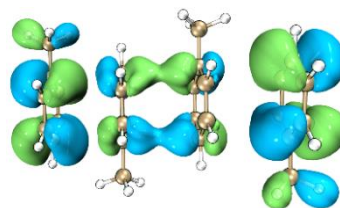
FFFF   SOMO   HDMO
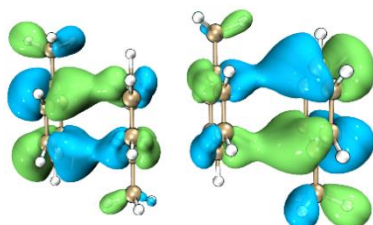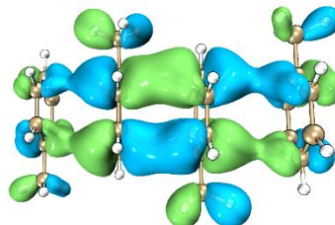
HDMO-1   HDMO-4
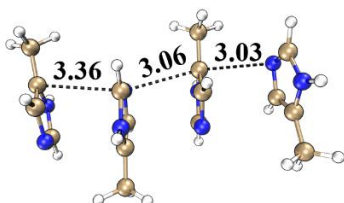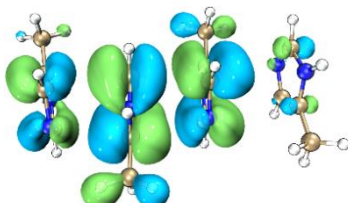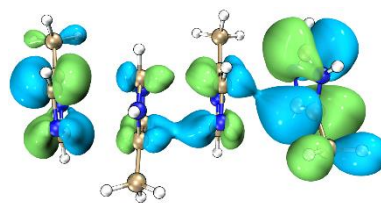
HHHH   SOMO   HDMO
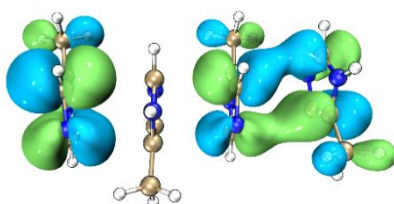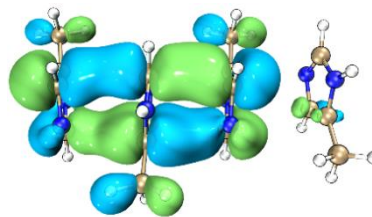
HDMO-1   HDMO-2
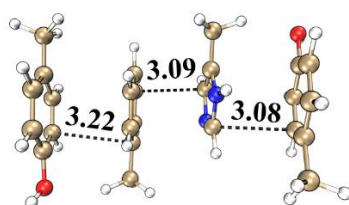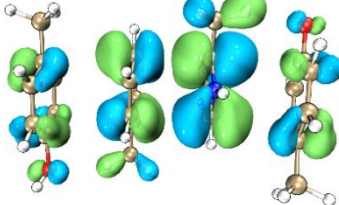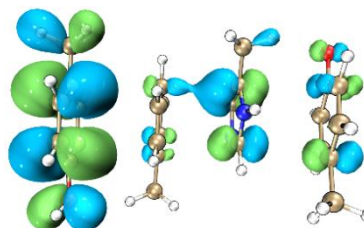
YFHY   SOMO   HDMO
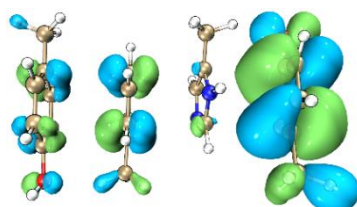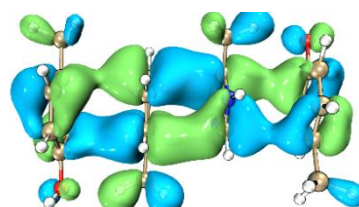
HDMO-1   HDMO-3
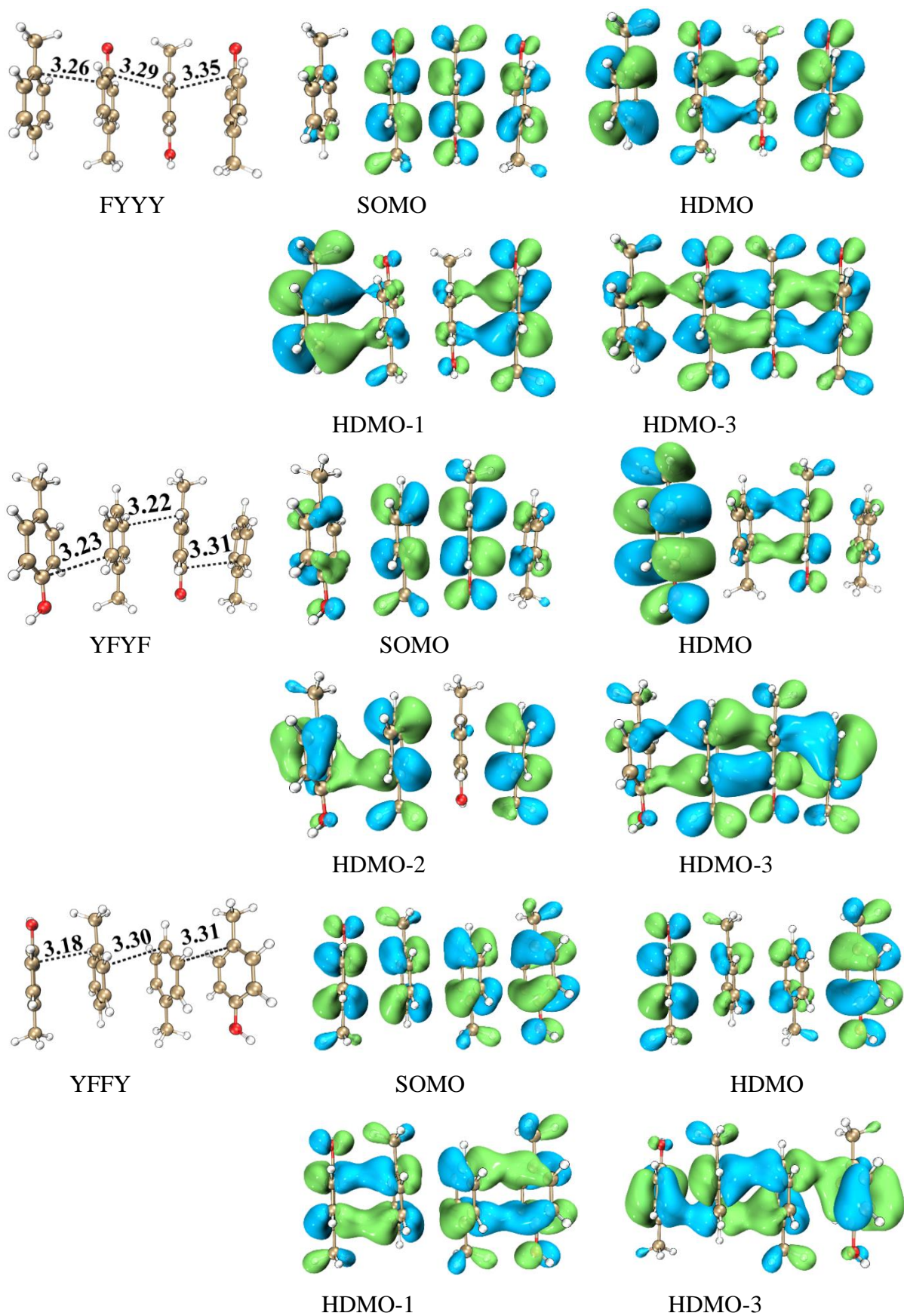
Figure S10. The structures of the $\pi{:}\pi{\therefore}\pi{:}\pi{\leftrightarrow}\pi{:}\pi{:}\pi{\therefore}\pi$ four-π seven-electron bindingf for the simple models with the corresponding front MOs.

HHHHH   SOMO   HDMO-2

HDMO-3

FFFFF   SOMO   HDMO-1

HDMO-4   HDMO-6

FFFFFF   SOMO   HDMO-3

HDMO-6   HDMO-8
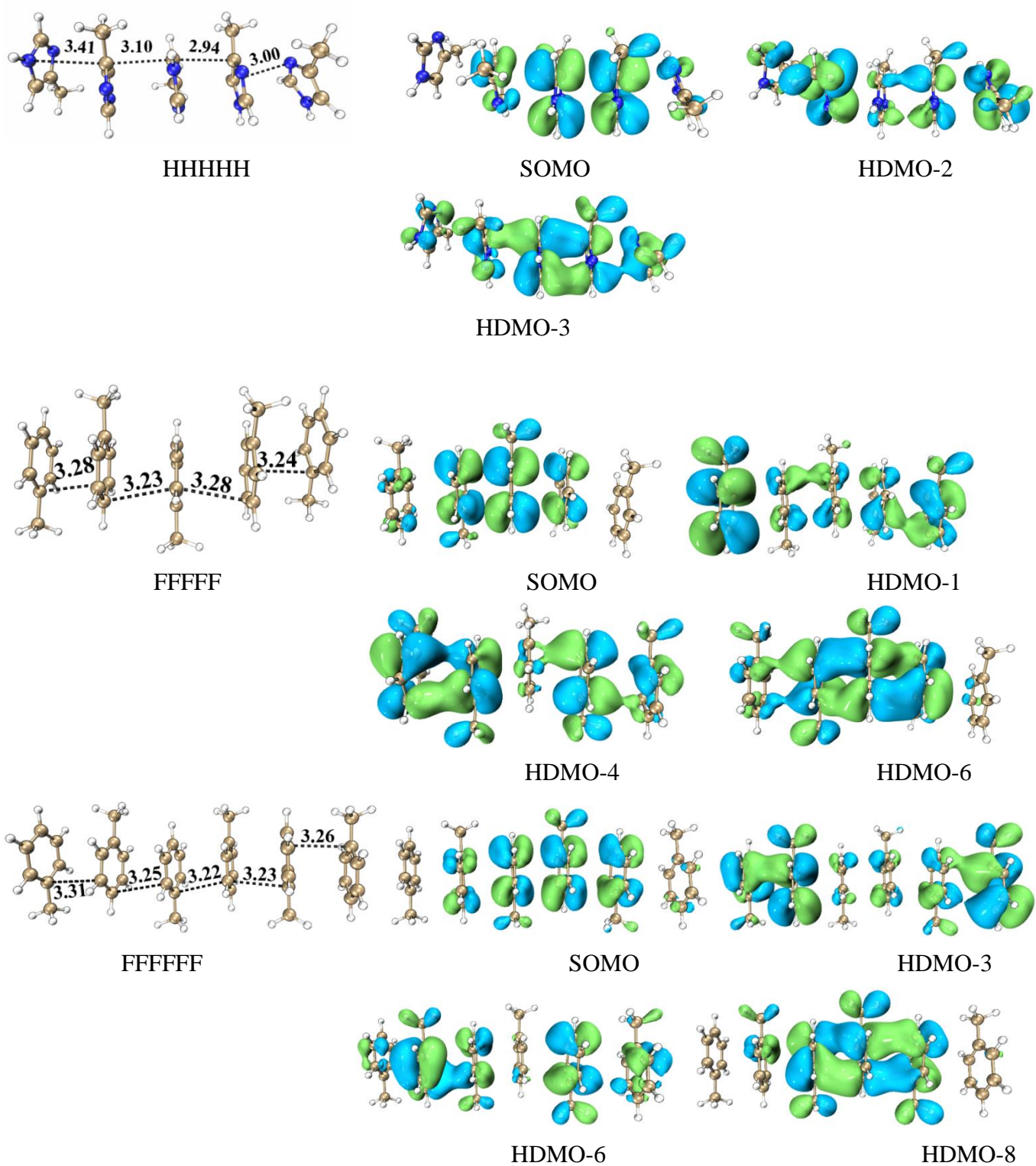
Figure S11. The structures of the five-π and six-π stacking systems for the simple models with the corresponding front MOs.

FHF-p   SOMO   HDMO   HDMO-3

YHF-p   SOMO   HDMO   HDMO-2/3

FYY-p   SOMO   HDMO   HDMO-1/4

HYY-p   SOMO   HDMO   HDMO-1

YHY-p   SOMO   HDMO   HDMO-1

YYY-p   SOMO   HDMO   HDMO-1

FFFF-p   SOMO   HDMO-2   HDMO-8

YYFY-p   SOMO   HDMO-1   HDMO-2
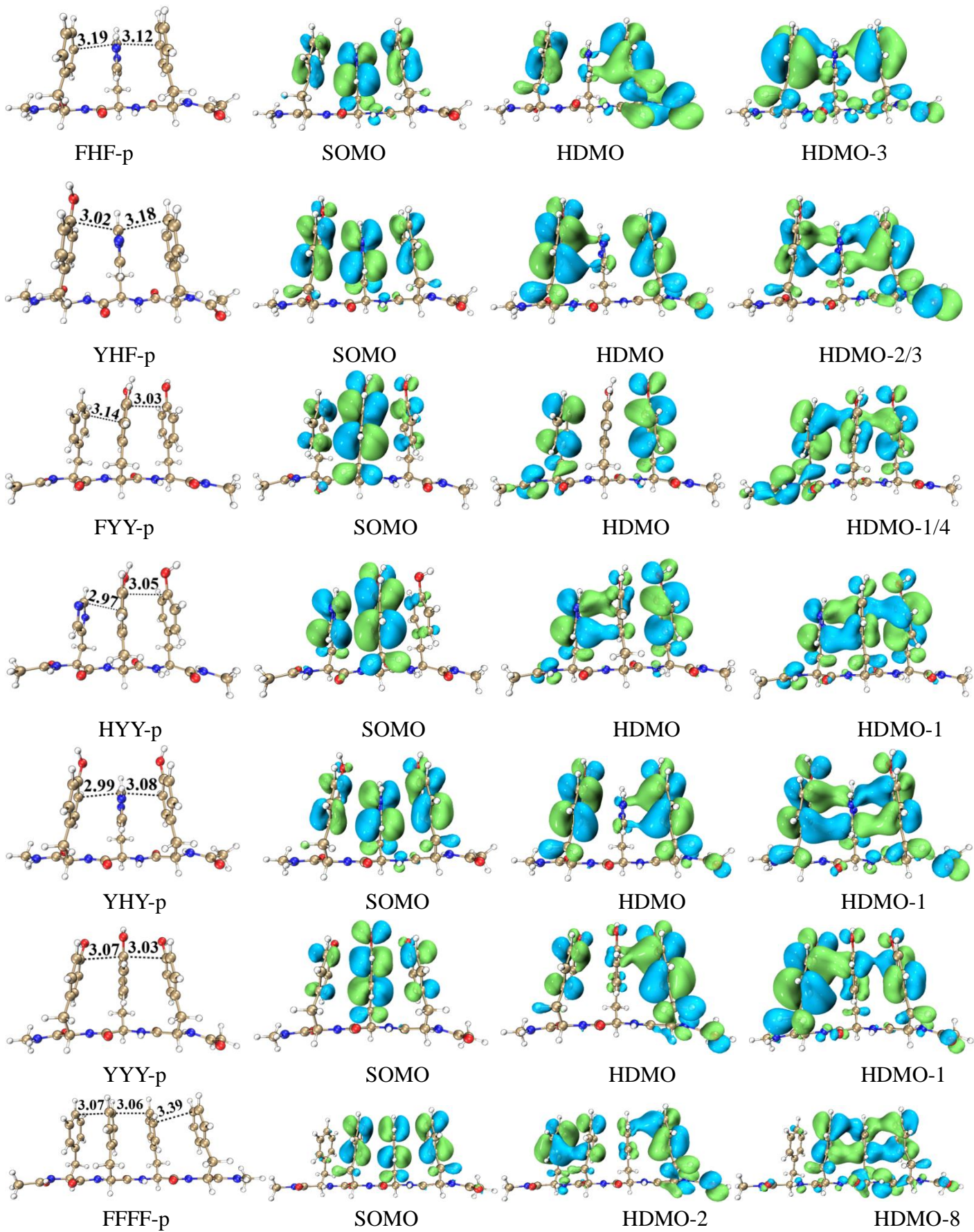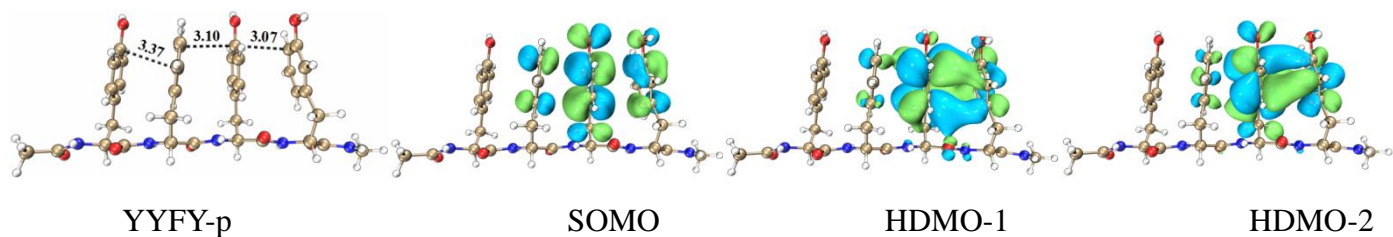
Figure S12. The structures of one-chain models and the corresponding SOMO, HDMO and HDMO-X.

FPheF   SOMO   HDMO   HDMO-2

FPheF-1   SOMO   HDMO   HDMO-5

FHisH   SOMO   HDMO   HDMO-1   HDMO-2

FTyrH   SOMO   HDMO   HDMO-1
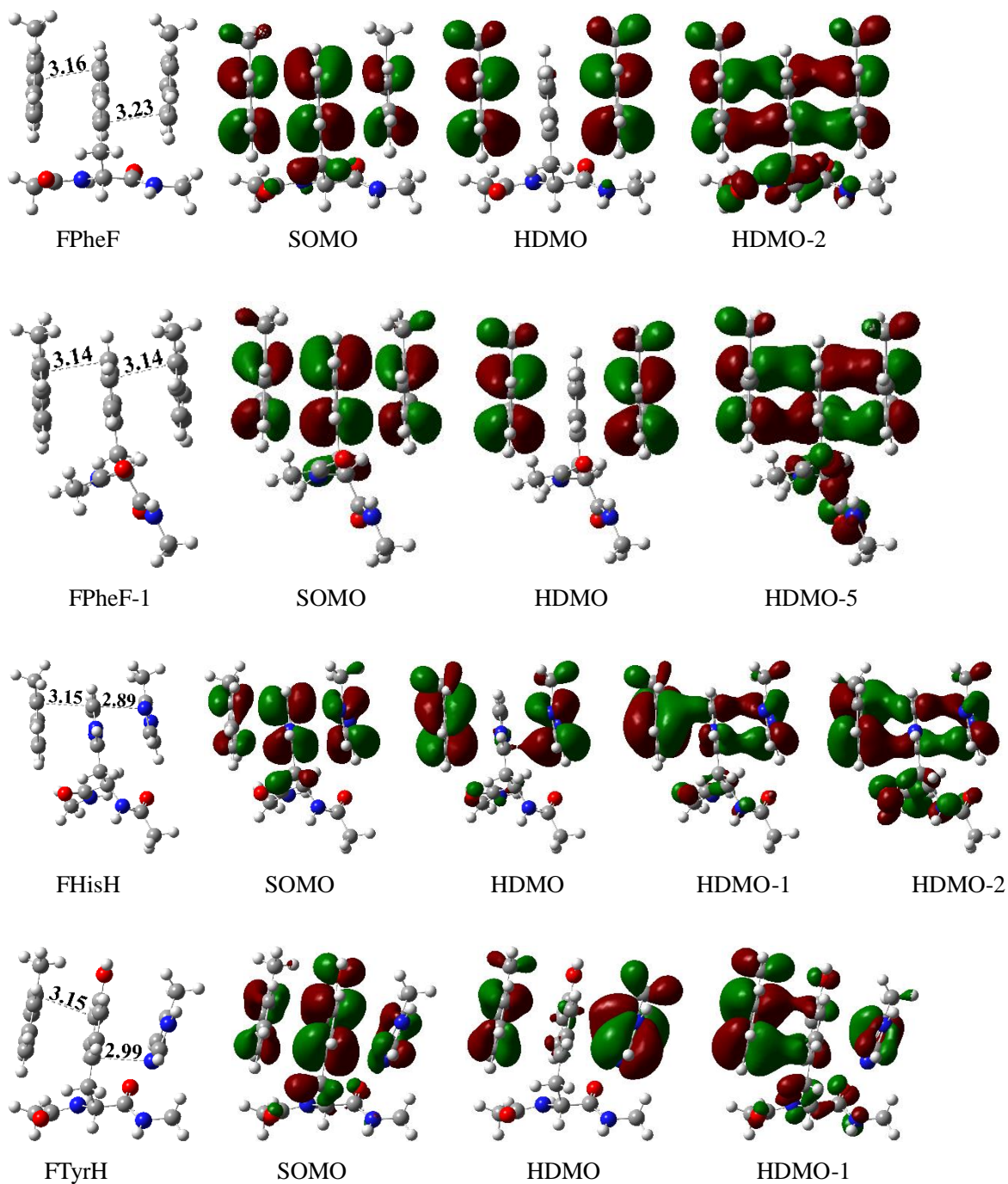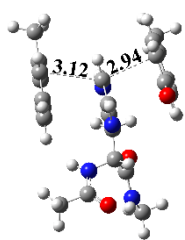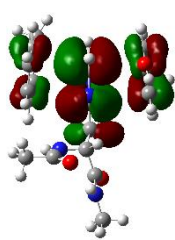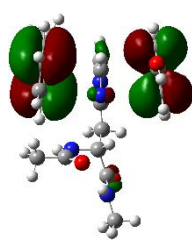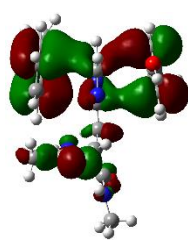
FHisY   SOMO   HDMO-4   HDMO-6
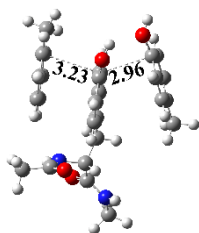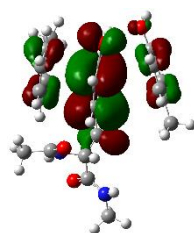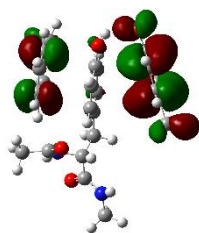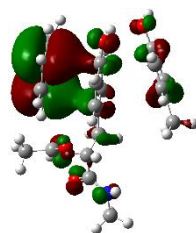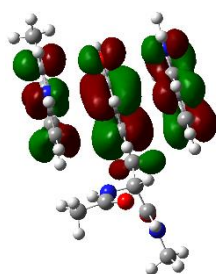
FTyrY   SOMO   HDMO   HDMO-2
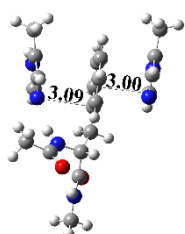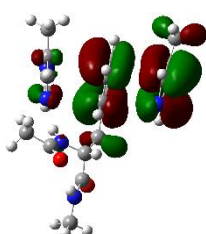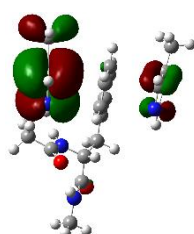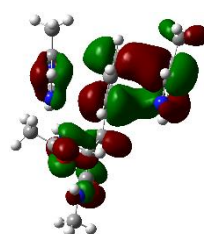
HPheH   SOMO   HDMO-2   HDMO-4
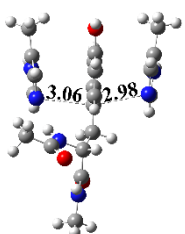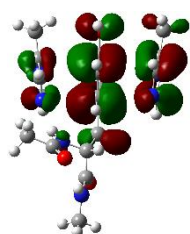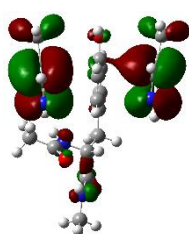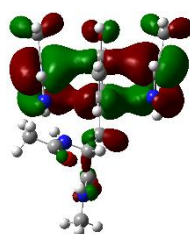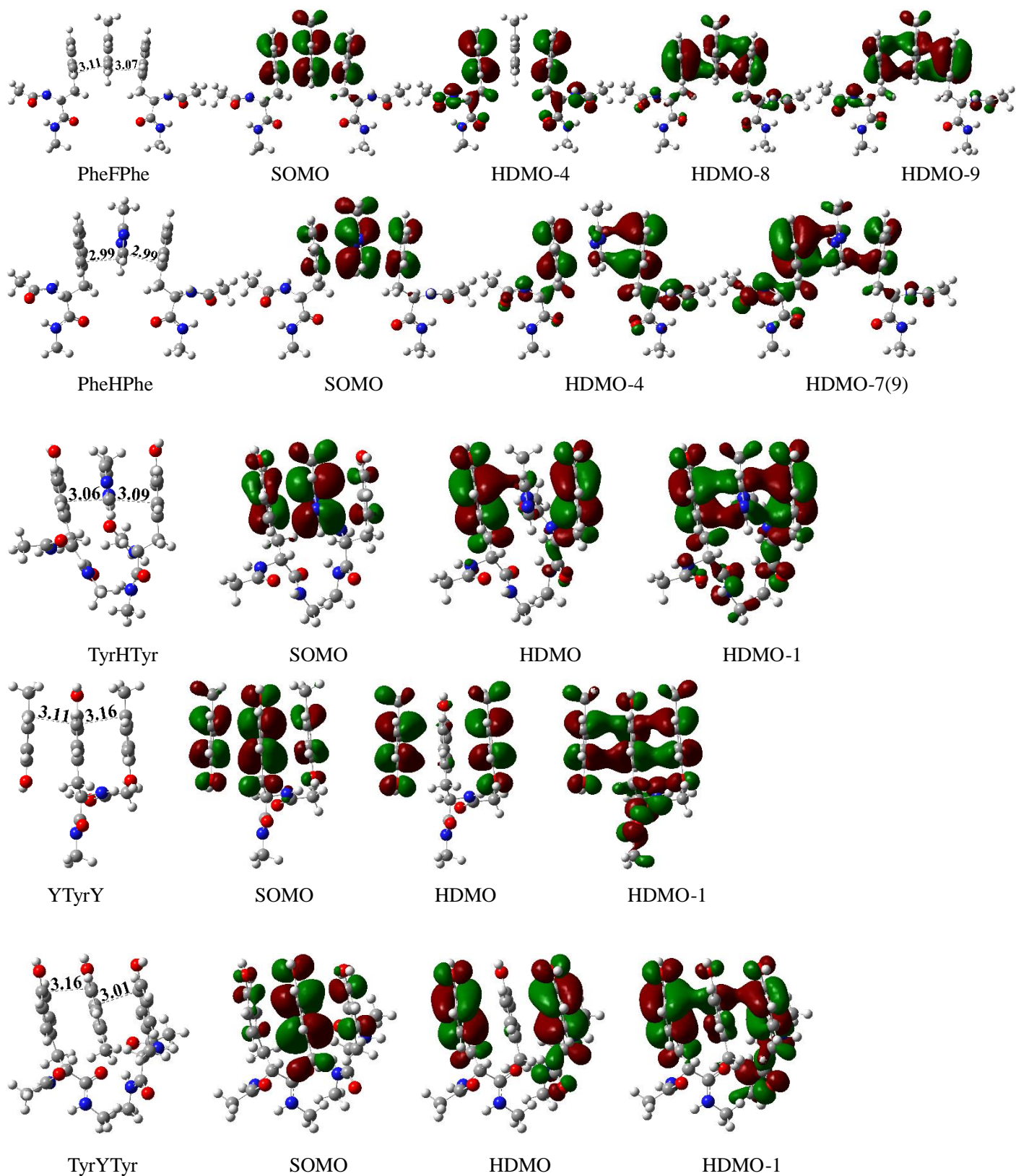
HTyrH   SOMO   HDMO-2   HDMO-3
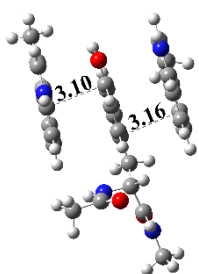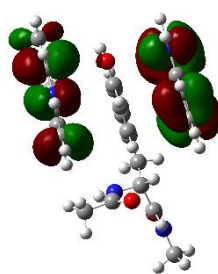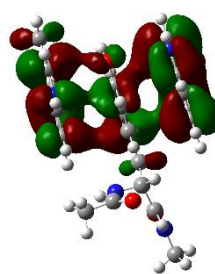
WTyrW   SOMO   HDMO   HDMO-1

Figure S13. The cases for the formations of $\pi\therefore\pi{:}\pi\leftrightarrow\pi{:}\pi\therefore\pi$ binding in proteins with three aromatic side chains in different peptide chains.